PRAMANA
— journal of
physics

Vol. 74, No. 4
April 2010
pp. 541–553

The investigation of $0^+ \leftrightarrow 0^- \beta$ decay in some spherical nuclei

NECLA CAKMAK[1,*], KAAN MANISA[2], SERDAR UNLU[3] and CEVAD SELAM[4]
[1]Department of Physics, Karabuk University, Karabuk, Turkey
[2]Department of Physics, Dumlupinar University, Kutahya, Turkey
[3]Department of Physics, Mehmet Akif Ersoy University, Burdur, Turkey
[4]Department of Physics, Anadolu University, Eskisehir, Turkey
[*]Corresponding author. E-mail: neclac@karabuk.edu.tr

MS received 19 August 2009; revised 19 November 2009; accepted 22 December 2009

Abstract. The $0^+ \leftrightarrow 0^-$ first-forbidden β decay transitions have been investigated for some spherical nuclei. The theoretical framework is based on a proton–neutron quasiparticle random phase approximation (pnQRPA). The Woods–Saxon potential basis has been used in our calculations. The transition probabilities have been calculated within the ξ approximation. The relativistic β moment matrix element has been calculated both directly without any assumption and assuming that it is proportional to the non-relativistic one.

Keywords. First-forbidden β decay; proton–neutron quasiparticle random phase approximation; shell model.

PACS Nos 23.40.Bw; 23.40.-s; 23.40.Hc

1. Introduction

It is well known that β decay processes are very important to understand the weak interaction processes and the nuclear structure. Although there are many theoretical and experimental studies about the allowed β transitions in literature, scientists have not shown the same interest in forbidden transitions. The studies performed recently show that the first-forbidden β transition process provides useful information in checking the validity of theories related to the r-processes and $2\nu\beta\beta$ [1–10]. The β decay rates have been calculated using continuum quasiparticle random phase approximation (CQRPA) method in ref. [1]. A systematic study of the total β decay half-lives and delayed neutron emission probabilities has been performed by considering the Gammow–Teller (GT) and first-forbidden transitions. Due to the shell configuration effects, the first-forbidden decays have a strong impact on the β decay characteristics of the r-process of the relevant nuclei with $Z \approx 28$, $N > 50$; $Z \geq 50$, $N > 82$ and $Z = 60$–70, $N \approx 126$. Suppression of the delayed

neutron emission probability has been found in nuclei with the neutron excess bigger than one major shell. The effect originates from the high-energy first-forbidden transitions to states outside the $(Q_\beta - B_n)$ window in the daughter nuclei. Borzov studied GT and first-forbidden decays near the r-process paths at $N = 50, 82$ and 126 by using density functional + CQRPA approach [2,3]. The model developed here provides a framework for microscopic global calculations of the GT and first-forbidden decays for the r-process relevant nuclei. The effect of the high-energy first-forbidden transitions is found to be decisive in $Z \geq 50$, $N \approx 82$ region and also in the $N = 126$ region.

The first-forbidden β decay may also have a significant role in the study of $2\nu\beta\beta$. The use of intermediate virtual excitations, other than the allowed ones, has been advocated by some scientists [4,5] even though the leptonic wave functions, for a single vertex, would include terms which are proportional to the product of the electron or neutrino momentum and the nuclear radius [6]. As a consequence, their contributions to the second-order process, which implies the product of two of such vertex functions, would be severely suppressed [7]. Civitarese and Suhonen studied the contributions of unique first-forbidden transitions to two-neutrino double β decay half-lives for ^{76}Ge $\rightarrow$ ^{76}Se transitions [9]. They considered only the contributions of 2^- excited states to the half-live values. The results of the pnQRPA calculations show that these transitions cannot contribute to the $2\nu\beta\beta$ process since their matrix elements are too small to compensate for the strong suppression of the decay rate by the corresponding leptonic phase-space factors. Unlu *et al* have calculated the $2\nu\beta\beta$ nuclear matrix elements for ^{128,130}Te $\rightarrow$ ^{128,130}Xe transitions [10]. Although all the contributions coming from the allowed β transitions are included in these calculations, the matrix element values are found to be smaller than the corresponding experimental values. It can be said that the consideration of the possible contributions from the first-forbidden β transitions will make the matrix element values closer to the corresponding experimental values.

Civitarese *et al* [11] studied the effect of spin–isospin-dependent interactions on the observable of the low-energy first-forbidden β decay transitions between double-odd and double-even nuclei with $|\Delta J| = 0, 2$. The matrix element of the relativistic β moment $M^{\pm}(\rho_A, \lambda = 0)$ has not been calculated analytically, but assumed to be proportional to the matrix element of non-relativistic β moment $iM^{\pm}(j_A, k = 1, \lambda = 0)$. They calculated the ft values for the ground state-to-ground state transitions with $\Delta J = 0, 2$. The ft values obtained for $\Delta J = 0$ showed a good agreement with the corresponding experimental data. However, the ft values obtained for $\Delta J = 2$ showed a good agreement only when the spin–isospin-dependent residual interactions were included. The energy of the first-forbidden resonance is in agreement with previously reported experimental and model estimates. The calculations were based on the single-particle states with the energies given by Nilsson's harmonic oscillator parametrizations. Suhonen studied the β decay properties for ^{136}I(2^-) $\rightarrow$ ^{136}Xe(J^π) and ^{136}Cs(5^+) $\rightarrow$ ^{136}Ba(J^π), as well as the β^+/EC transitions ^{136}La(1^+) $\rightarrow$ ^{136}Ba(J^π) [12]. The β decay transitions were treated in their allowed and first-forbidden approximations including also the ground state transition. The detailed β decay properties from an odd–odd nucleus to the excited states of the adjacent even–even nucleus were studied within the framework of QRPA assuming that a common vacuum and the harmonic oscillator

basis were used in the calculations. De Witte *et al* observed β decay for neutron-rich ^{218}Bi isotope by the pulsed-release technique and resonant laser ionization [13]. The half-life value for the transition was obtained and a level scheme was constructed for the ^{218}Po daughter. The experimental half-life was compared with the self-consistent CQRPA calculations and a satisfactory agreement was reached when the first-forbidden transitions were included. First-forbidden β decay observable and other related weak-interaction variables were studied in ref. [14]. The calculations were presented for four relatively strong first-forbidden β decays in the mass region of $A = 11$–16 in order to study the very large mesonic-exchange-current enhancement of the rank-zero components. Baumann *et al* studied $^{50}\mathrm{K}(0^-) \rightarrow {}^{50}\mathrm{Ca}(0^-)$ transition [15] and it was concluded that this decay provides the best case for interpreting the effects of meson exchange enhancement, because both the $p_{3/2}$ neutron and $d_{3/2}$ proton states are at the Fermi surface in ^{50}K, with the result that the wave functions for ^{50}K and ^{50}Ca are rather simple and dominated by components which give a large first-forbidden matrix element.

In refs [16,17], the $0^+ \leftrightarrow 0^-$ first-forbidden β decay has been searched for $^{206-214}\mathrm{Pb} \rightarrow {}^{206-214}\mathrm{Bi}$ transitions. The calculations have been performed according to two different approximations. In the first approximation, the relativistic β transition operator has been calculated directly without any assumption. Secondly, the relativistic operator has been assumed to be proportional to the non-relativistic one. However, the contribution of the spin-orbit term in the shell model potential has been neglected in the calculation of the relativistic part of the first-forbidden β decay matrix element. In the present study, the $0^+ \leftrightarrow 0^-$ first-forbidden β transitions have been investigated for the spherical nuclei in the mass region of $90 \leq A \leq 214$. The relativistic part of the first-forbidden β decay matrix element has been calculated directly without any assumption. The difference of our calculations from the calculations in refs [16,17] is the inclusion of the contribution coming from the spin-orbit potential in the calculation of the relativistic matrix element. The calculations have been performed within the framework of the pnQRPA method with the separable residual effective interactions in the particle–hole (ph) and the particle–particle (*pp*) channel. Thus, the influence of the *pp* interaction on the calculated $\log ft$ values has been studied for the nuclei under consideration.

2. Theoretical formalism

The model Hamiltonian which generates the spin–isospin-dependent vibration modes with $I^\pi = 0^-$ in odd–odd nuclei in quasiboson approximation is given as follows:

$$\hat{H} = \hat{H}_{\mathrm{SQP}} + \hat{h}_{ph} + \hat{h}_{pp}. \tag{1}$$

The single quasiparticle (SQP) Hamiltonian of the system is given by

$$\hat{H}_{\mathrm{SQP}} = \sum_{j_k} \varepsilon_{j_k} \alpha^\dagger_{j_\tau m_\tau} \alpha_{j_\tau m_\tau} (\tau = p, n), \tag{2}$$

where ε_{j_k} is the single quasiparticle energy of the nucleons with angular momentum j_k, and $\alpha^\dagger_{j_\tau m_\tau}$ ($\alpha_{j_\tau m_\tau}$) is the quasiparticle creation (annihilation) operator.

The $\hat{h}_{ph}$ and $\hat{h}_{pp}$ are the spin–isospin effective interaction Hamiltonians which generate 0^- vibration modes in *ph* and *pp* channels, respectively and given as

$$\hat{h}_{ph} = \frac{2\chi_{ph}}{g_A^2} \sum_{j_p j_n j_{p'} j_{n'}} [b_{j_p j_n} A^\dagger_{j_p j_n} + \bar{b}_{j_p j_n} A_{j_p j_n}] \cdot [b_{j_{p'} j_{n'}} A_{j_{p'} j_{n'}} + \bar{b}_{j_{p'} j_{n'}} A^\dagger_{j_{p'} j_{n'}}] \quad (3)$$

$$\hat{h}_{pp} = \frac{2\chi_{pp}}{g_A^2} \sum_{j_p j_n j_{p'} j_{n'}} [p_{j_p j_n} A^\dagger_{j_p j_n} - \bar{p}_{j_p j_n} A_{j_p j_n}] \cdot [p_{j_{p'} j_{n'}} A_{j_{p'} j_{n'}} - \bar{p}_{j_{p'} j_{n'}} A^\dagger_{j_{p'} j_{n'}}], \quad (4)$$

where χ_{ph} and χ_{pp} are the *ph* and *pp* effective interaction constants, respectively.

The quasiboson creation $A^\dagger_{j_p j_n}$ and annihilation $A_{j_p j_n}$ operators are given as follows:

$$A^\dagger_{j_p j_n} = \frac{1}{\sqrt{2j+1}} \sum_m (-1)^{j-m} \alpha^\dagger_{j_p m_p} \alpha_{j_n - m_n} \quad (5)$$

$$A_{j_p j_n} = (A^\dagger_{j_p j_n})^\dagger. \quad (6)$$

$b_{j_p j_n}, \bar{b}_{j_p j_n}, p_{j_p j_n}$ and $\bar{p}_{j_p j_n}$ are the reduced matrix elements of the non-relativistic multipole operators [18].

$$iM^{\mp}(j_A, \kappa = 1, \lambda = 0) = g_A \sum_{k=1}^{A} t_{\mp}(k) r_k [Y_1(r_k)\sigma(k)]_0 \quad (7)$$

and designed by

$$b_{j_p j_n} = \langle j_p(l_p s_p) \| r[Y_1 \sigma]_0 \| j_n(l_n s_n) \rangle V_{j_n} U_{j_p},$$

$$\bar{b}_{j_p j_n} = \langle j_p(l_p s_p) \| r[Y_1 \sigma]_0 \| j_n(l_n s_n) \rangle U_{j_n} V_{j_p},$$

$$p_{j_p j_n} = \langle j_p(l_p s_p) \| r[Y_1 \sigma]_0 \| j_n(l_n s_n) \rangle U_{j_p} U_{j_n},$$

$$\bar{p}_{j_p j_n} = \langle j_p(l_p s_p) \| r[Y_1 \sigma]_0 \| j_n(l_n s_n) \rangle V_{j_p} V_{j_n},$$

where U_{j_τ} and V_{j_τ} are the standard BCS occupation amplitudes.

The Hamiltonian eq. (1) can be linearized using the pnQRPA. Therefore, charge-exchange 0^- vibration modes in odd–odd nuclei are considered as the phonon excitations and described by

$$|\Psi_i\rangle = \hat{Q}^\dagger_i |0\rangle = \sum_j [\psi^i_{j_p j_n} \hat{A}^\dagger_{j_p j_n} - \varphi^i_{j_p j_n} \hat{A}_{j_p j_n}] |0\rangle, \quad (8)$$

where $\hat{Q}^\dagger_i$ is the pnQRPA phonon creation operator, $|0\rangle$ is the phonon vacuum which corresponds to the ground state of an even–even nucleus and fulfills $\hat{Q}_i|0\rangle = 0$ for

all i. $\psi^i_{j_pj_n}$ and $\varphi^i_{j_pj_n}$ are forward and backward quasiboson amplitudes, respectively. Assuming that the phonon operators obey the commutation relations given below,

$$\langle 0|[\hat{Q}_i, \hat{Q}^\dagger_j]|0\rangle = \delta_{ij}, \tag{9}$$

$$\langle 0|[\hat{Q}_i, \hat{Q}_j]|0\rangle = 0, \tag{10}$$

we obtain the following orthonormalization condition for quasiboson amplitudes $\psi^i_{j_pj_n}$ and $\varphi^i_{j_pj_n}$:

$$\sum_j [\psi^i_{j_pj_n}\psi^{i'}_{j_pj_n} - \varphi^i_{j_pj_n}\varphi^{i'}_{j_pj_n}] = \delta_{ii'}. \tag{11}$$

Employing the conventional procedure of pnQRPA and solving the equation of motion

$$[\hat{H}, \hat{Q}^\dagger_j]|0\rangle = \omega_i \hat{Q}^\dagger_j|0\rangle \tag{12}$$

the pnQRPA equations take the form

$$\sum_{np} [\rho_{npn'p'}\psi^i_{j_pj_n} - \eta_{npn'p'}\varphi^i_{j_pj_n}] = \omega_i \psi^i_{j_pj_n}, \tag{13}$$

$$\sum_{np} [\eta_{npn'p'}\psi^i_{j_pj_n} - \rho_{npn'p'}\varphi^i_{j_pj_n}] = \omega_i \varphi^i_{j_pj_n}, \tag{14}$$

where

$$\begin{aligned}\rho_{npn'p'} &= E_{np}\delta_{nn'}\delta_{pp'} \\ &\quad +2[\chi_{ph}(b_{np}b_{n'p'} + \bar{b}_{np}\bar{b}_{n'p'}) + \chi_{pp}(d_{np}d_{n'p'} + \bar{d}_{np}\bar{d}_{n'p'})]\end{aligned}$$

and

$$\begin{aligned}\eta_{npn'p'} &= -2[\chi_{ph}(\bar{b}_{np}b_{n'p'} + b_{np}\bar{b}_{n'p'}) + \chi_{pp}(\bar{d}_{np}d_{n'p'} + d_{np}\bar{d}_{n'p'})] \\ d_{j_pj_n} &= \langle j_p(l_ps_p)\|\frac{1}{\sqrt{4\pi}c}(\vec{\sigma}\cdot\vec{V})\|j_n(l_ns_n)\rangle V_{j_n}U_{j_p} \\ \bar{d}_{j_pj_n} &= \langle j_p(l_ps_p)\|\frac{1}{\sqrt{4\pi}c}(\vec{\sigma}\cdot\vec{V})\|j_n(l_ns_n)\rangle U_{j_n}V_{j_p}.\end{aligned}$$

ω_i is the ith 0^- excitation energy in odd–odd nuclei calculated from the ground state of the parent even–even nucleus. Excitation energies ω_i and $\psi^i_{j_pj_n}$, $\varphi^i_{j_pj_n}$ amplitudes are found from eqs (11), (13) and (14).

3. The calculation of matrix elements

The calculation of the transition probabilities for $0^+ \leftrightarrow 0^-$ transitions has been performed using the ξ approximation. This approximation is fairly accurate for the investigated transitions, but it is important in the quantitative evaluation of the multipole moments to include the corrections due to the finite nuclear size (see ref. [18] to get a detailed information about the ξ approximation).

The transition probabilities $B(0^+ \rightarrow 0_i^-, \beta^{\mp})$ in ξ approximation are given by [18]

$$B(0^+ \rightarrow 0_i^-, \beta^{\mp}) = |\langle 0_i^- \| M_{\beta^{\mp}} \| 0^+ \rangle^2, \tag{15}$$

where

$$M_{\beta^{\mp}} = \pm M^{\mp}(\rho_A, \lambda = 0) - i\frac{m_e c}{\hbar}\xi M^{\mp}(j_A, \kappa = 1, \lambda = 0) \tag{16}$$

and $M^{\mp}(\rho_A, \lambda = 0)$ are relativistic first-forbidden β decay multipole operators [18].

$$M^{\mp}(\rho_A, \lambda = 0) = \frac{g_A}{c\sqrt{4\pi}}\Sigma_k t_{\mp}(k)(\vec{\sigma}(k) \cdot \vec{V}(k)). \tag{17}$$

In eq. (16), the upper and lower signs refer to β^- and β^+ decays, respectively.

The reduced matrix elements $\langle 0_i^- \| M_{\beta^{\mp}} \| 0^+ \rangle$ in the framework of the pnQRPA are given as

$$\langle 0_i^- | M_{\beta^-} | 0^+ \rangle = \langle 0^+ | [Q_i, M_{\beta^-}] | 0 \rangle = \sum_{j_p j_n} (b_{j_p j_n} \psi^i_{j_p j_n} + \bar{b}_{j_p j_n} \varphi^i_{j_p j_n}) \tag{18}$$

$$\langle 0_i^- | M_{\beta^+} | 0^+ \rangle = \langle 0^+ | [Q_i, M_{\beta^+}] | 0 \rangle = \sum_{j_p j_n} (\bar{b}_{j_p j_n} \psi^i_{j_p j_n} + b_{j_p j_n} \varphi^i_{j_p j_n}). \tag{19}$$

The ft values are given by the following expression:

$$(ft)_{\beta^{\mp}} = \frac{D}{(g_A/g_V)^2 4\pi B(I_i \rightarrow I_f, \beta^{\mp})}, \tag{20}$$

where

$$D = \frac{2\pi^3 \hbar^2 \ln 2}{g_V^2 m_e^5 c^4} = 6250 \text{ s}, \quad \frac{g_A}{g_V} = -1.24 \text{ [14]}.$$

4. Results and discussions

The $0^+ \leftrightarrow 0^-$ first-forbidden $\beta^{\mp}$ decay transitions have been investigated for some nuclei in the mass range of $90 \leq A \leq 214$. The relativistic matrix elements of the first-forbidden β decay operators have been calculated without any assumption. A comparison of the calculated values with those calculated by assuming that the

Table 1. The relativistic reduced quasiparticle matrix elements.

		$\langle I_f \| T^{\mp}_{\rm rel} \| I_i \rangle$			
		Proportional to Λ_0		Direct calculation	
Transition	Single particle transition	[11]	C2	[16]	C1
^{96}Y → ^{96}Zr	$(3s^n_{1/2}–2p^p_{1/2})$	0.075	0.027	0.081	0.080
^{120}Xe → ^{120}I	$(3s^n_{1/2}–2p^p_{1/2})$	0.067	0.099	0.075	0.075
^{140}Ba → ^{140}La	$(2f^n_{7/2}–1g^p_{7/2})$	0.018	0.063	0.299	0.297
^{144}Ce → ^{144}Pr	$(2f^n_{7/2}–1g^p_{7/2})$	0.023	0.074	0.299	0.297
^{144}Pr → ^{144}Nd	$(2f^n_{7/2}–1g^p_{7/2})$	0.176	0.057	0.294	0.288
^{206}Hg → ^{206}Tl	$(3p^n_{1/2}–3s^p_{1/2})$	0.214	0.160	0.087	0.085
^{206}Tl → ^{206}Pb	$(3p^n_{1/2}–3s^p_{1/2})$	0.198	0.063	0.084	0.082
^{210}Pb → ^{210}Bi	$(2g^n_{9/2}–1h^p_{9/2})$	0.099	0.117	0.379	0.374
^{212}Pb → ^{212}Bi	$(2g^n_{9/2}–1h^p_{9/2})$	0.143	0.158	0.381	0.376
^{214}Pb → ^{214}Bi	$(2g^n_{9/2}–1h^p_{9/2})$	0.172	0.187	0.382	0.378

Table 2. The $\log ft$ values obtained by directly calculating the relativistic matrix elements.

	$\log ft$		
Transition	Exp. [20]	$\chi_{pp=0}$	$\chi_{pp\neq 0}$
^{90}Kr → ^{90}Rb	5.91	5.64	5.64
^{92}Rb → ^{92}Sr	6.03	4.80	4.79
^{96}Y → ^{96}Zr	5.70	5.15	5.14
^{98}Y → ^{98}Zr	5.80	5.21	5.20
^{120}Xe → ^{120}I	6.00	4.95	4.94
^{142}Ce → ^{142}Pr	5.60	5.97	5.96
^{144}Pr → ^{144}Nd	6.53	4.89	4.88
^{194}Pb → ^{194}Tl	5.65	4.45	4.44
^{196}Pb → ^{196}Tl	6.34	4.52	4.51
^{200}Pb → ^{200}Tl	6.11	5.35	5.37
^{206}Hg → ^{206}Tl	5.42	7.20	7.19
^{206}Tl → ^{206}Pb	5.17	4.75	4.74
^{210}Pb → ^{210}Bi	5.50	5.43	5.44
^{212}Pb → ^{212}Bi	5.19	5.13	5.14
^{214}Pb → ^{214}Bi	5.05	4.95	4.94

relativistic matrix elements are proportional to the non-relativistic matrix elements has been given in this section. The *pp* term of β decay effective interaction has also been considered in the investigation of 0^- excited state in odd–odd nucleus. Hence, the effect of the *pp* interaction on the β decay $\log ft$ values could be searched for the nuclei in the mentioned region.

Table 3. The log ft values obtained by assuming that the relativistic matrix elements are proportional to Λ_0.

	log ft		
Transition	Exp. [20]	$\chi_{pp=0}$	$\chi_{pp\neq 0}$
^{90}Kr → ^{90}Rb	5.91	5.78	5.77
^{92}Rb → ^{92}Sr	6.03	5.98	5.97
^{96}Y → ^{96}Zr	5.70	5.83	5.82
^{98}Y → ^{98}Zr	5.80	5.92	5.91
^{120}Xe → ^{120}I	6.00	5.40	5.39
^{142}Ce → ^{142}Pr	5.60	5.79	5.78
^{144}Pr → ^{144}Nd	6.53	5.45	5.44
^{194}Pb → ^{194}Tl	5.65	4.82	4.81
^{196}Pb → ^{196}Tl	6.34	4.88	4.87
^{200}Pb → ^{200}Tl	6.11	5.38	5.40
^{206}Hg → ^{206}Tl	5.42	4.97	4.96
^{206}Tl → ^{206}Pb	5.17	4.98	4.97
^{210}Pb → ^{210}Bi	5.50	5.15	5.14
^{212}Pb → ^{212}Bi	5.19	4.87	4.88
^{214}Pb → ^{214}Bi	5.05	4.75	4.74

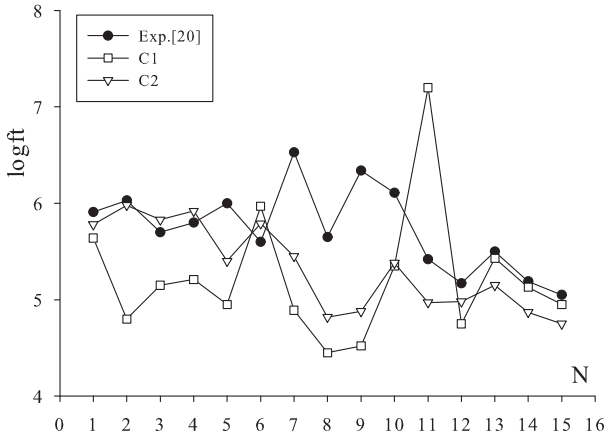

Figure 1. The first-forbidden β transition log ft values.

The theoretical formalism is based on the pnQRPA method. In numerical calculations, the Woods–Saxon potential with Chepurinov parametrization [19] has been used. The basis contains all discrete and quasistationary states, and all the neutron and proton transitions changing the radial quantum number by $\Delta n = 0, 1, 2, 3$ have been included. The values of the pair correlation constants have been taken as $C_n = C_p = 12/\sqrt{A}$ for open shell nuclei. The parameters of the effective interaction are $\chi_{ph} = 30A^{-5/3}$ MeV fm^{-2} and $\chi_{pp} = 0.1 \times \chi_{ph}$ MeV fm^{-2}.

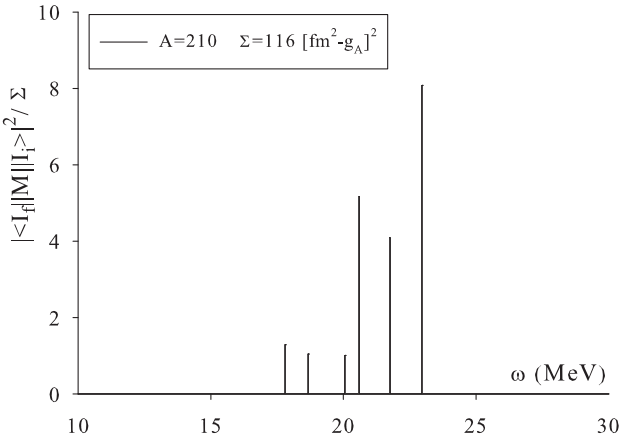

Figure 2. The first-forbidden β transition strength distribution in ^{210}Pb.

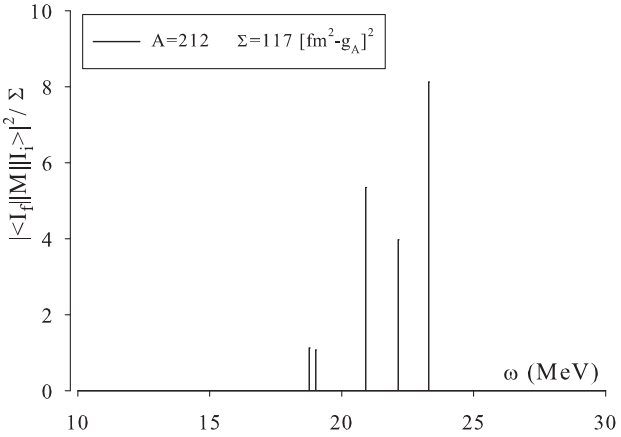

Figure 3. The first-forbidden β transition strength distribution in ^{212}Pb.

The single quasiparticle (SQP) values of the relativistic β transition operator, which have been calculated under different assumptions, have been obtained from eq. (17) and results are given in table 1. The first and last transition states are given in the second column, the values obtained by assuming that the relativistic matrix element is proportional to the non-relativistic matrix element are given in the third and fourth columns, and the values calculated directly from the relativistic β decay transition operator are given in the fifth and sixth columns in table 1. The constant ratio $\Lambda_0 = 2.4$ has been accepted in the calculations. The contribution of the spin-orbit term in the mean field potential has been neglected in the calculations of the fifth column of table 1, and considered in the calculations of the sixth column. It can be seen from table 1 that spin-orbit potential has a negligible effect on the matrix elements. However, there is an important difference between the calculated values of the relativistic matrix element without any assumption (C1) and the calculated

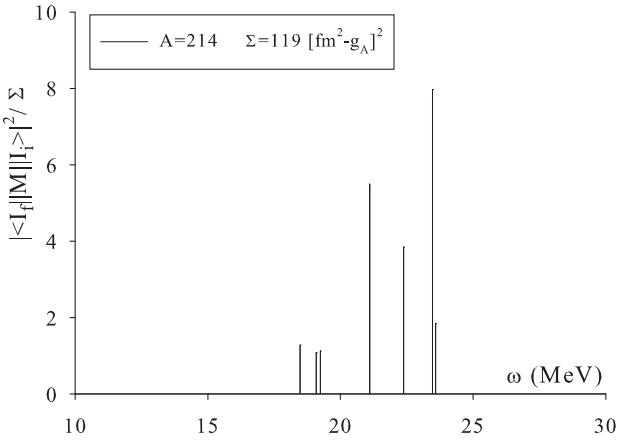

Figure 4. The first-forbidden β transition strength distribution in ^{214}Pb.

values based on the assumption that the relativistic matrix element is proportional to the non-relativistic one (C2). The results of C1 calculations except for the nuclei of ^{206}Hg $\rightarrow$ ^{206}Tl and ^{120}Xe $\rightarrow$ ^{120}I are bigger (2–5 times) than the results of C2 calculations.

The β decay $\log ft$ values for some $0^+ \leftrightarrow 0^-$ transitions in the mass region of $90 \leq A \leq 214$, which change between 5 and 6.5 experimentally, have been calculated using eq. (20). The results of C1 calculations obtained from eq. (17) have been compared with the experimental values in table 2. The $\log ft$ values of $\beta^{\mp}$ decay transitions have been calculated for the states of $\chi_{pp} = 0$ (fourth column) and $\chi_{pp} \neq 0$ (fifth column) to determine the influence of the *pp* interaction in the calculations. As seen from the table, the results are not affected by effective interaction in the *pp*-channel. Moreover, it can be said that the theoretical calculations are smaller than the experimental values. In fact, the theoretical $\log ft$ values are closer to the experimental values for the transitions ^{90}Kr $\rightarrow$ ^{90}Rb, ^{206}Tl $\rightarrow$ ^{206}Pb, $^{210-214}$Pb $\rightarrow$ $^{210-214}$Bi, in comparison with other transitions.

Also, the results of the C2 calculations have been compared with the experimental values in table 3. It can be clearly seen from table 3 that the effective interaction in the *pp*-channel has no considerable effect on the $\log ft$ values. The results of the C2 calculations are closer to the corresponding experimental values when compared with those of the C1 calculations. For example, the theoretical $\log ft$ values are closer to the experimental values for the transitions ^{90}Kr $\rightarrow$ ^{90}Rb, ^{92}Rb $\rightarrow$ ^{92}Sr, $^{96-98}$Y $\rightarrow$ $^{96-98}$Zr, ^{142}Ce $\rightarrow$ ^{142}Pr, ^{206}Tl $\rightarrow$ ^{206}Pb, $^{210-214}$Pb $\rightarrow$ $^{210-214}$Bi. Both the $\log ft$ values of calculations C1 and C2 are compared with the experimental values in figure 1. It can be seen from figure 1 that the values calculated using constant ratio Λ_0 for transitions 1–6 and the values directly calculated for transitions 13–15 are closer to the experimental values. Also, the results obtained by both methods for transitions 7–11 are smaller (1–1.5 units) than the experimental $\log ft$ values. The discrepancy in these transitions (7–11) can be attributed to the deformation of the nuclei under consideration, because our results have been calculated for mean field potential with spherical symmetry. Thus, we have shown that the results calculated

Table 4. The microscopic structure of the spectrum in figure 2.

ω_i (MeV)	Structure	ψ^i_{np}
17.80	$(2f^n_{5/2}–3d^p_{5/2})$	−0.99
	$(2g^n_{7/2}–1f^p_{7/2})$	−0.11
18.67	$(2d^n_{3/2}–3p^p_{3/2})$	−0.99
	$(3p^n_{3/2}–3d^p_{3/2})$	0.96
20.06	$(2d^n_{5/2}–2f^p_{5/2})$	−0.22
	$(2g^n_{9/2} - 1h^p_{9/2})$	−0.17
	$(1g^n_{9/2}–1h^p_{9/2})$	0.85
20.58	$(2d^n_{5/2}–2f^p_{5/2})$	0.39
	$(3p^n_{3/2}–3d^p_{3/2})$	0.23
	$(2f^n_{7/2}–2g^p_{7/2})$	0.19
	$(2f^n_{7/2}–2g^p_{7/2})$	0.96
21.75	$(1h^n_{11/2}–1i^p_{11/2})$	−0.25
	$(1g^n_{9/2}–1h^p_{9/2})$	0.12
	$(1h^n_{11/2}–1i^p_{11/2})$	0.96
22.96	$(2f^n_{7/2}–2g^p_{7/2})$	0.22
	$(1g^n_{9/2}–1h^p_{9/2})$	0.13

using constant ratio Λ_0 for transitions 1–6 (lighter nuclei) and the results directly calculated for transitions 13–15 are closer to experimental values.

The energy dependence of the strength distributions for the collective states in the lead region (for $^{210-214}$Pb isotopes) is shown in figures 2, 3 and 4. The dominant contributions are located at energies of the order (24–25) MeV which in our calculation represents the position of the giant first-forbidden resonance (FFR) with $I^\pi = 0^-$. For this mass region, the average energy of the 0^- giant FFR has been experimentally determined by Horen *et al* [21,22] at 25.3 MeV. As seen from figure 2, the energy of the associated giant FFR is found to be in agreement with the previously reported experimental [21,22] and model [11] estimates.

The $\psi^i_{j_n j_p}$ amplitudes of collective 0^- states are shown in tables 4–6. It can be seen from figures 2–4 that the giant FFR consists of these collective states. The collective 0^- states, composed of superpositions of pair of $(3p^n_{3/2}–3d^p_{3/2})$, $(2f^n_{7/2}–2g^p_{7/2})$, $(1g^n_{9/2}–1h^p_{9/2})$ and $(1h^n_{11/2}–1i^p_{11/2})$ are presented in these tables.

5. Conclusions

The $0^+ \leftrightarrow 0^-$ first-forbidden β decay transitions for some spherical nuclei have been investigated within the pnQRPA method. Two different approximations have been used in the calculation of the relativistic β decay matrix elements. Firstly, these matrix elements have been calculated without any assumption. Secondly,

Table 5. The microscopic structure of the spectrum in figure 3.

ω_i (MeV)	Structure	ψ^i_{np}
18.77	$(3p^n_{1/2}$–$4s^p_{1/2})$	−0.98
19.02	$(2d^n_{3/2}$–$3p^p_{3/2})$	−0.99
	$(1g^n_{9/2}$–$1h^p_{9/2})$	0.82
	$(2d^n_{5/2}$–$2f^p_{5/2})$	0.42
20.91	$(3p^n_{3/2}$–$3d^p_{3/2})$	0.29
	$(2f^n_{7/2}$–$2g^p_{7/2})$	0.18
	$(1h^n_{11/2}$–$1i^p_{11/2})$	−0.13
	$(2f^n_{7/2}$–$2g^p_{7/2})$	0.96
22.14	$(1i^n_{11/2}$–$1h^p_{11/2})$	−0.26
	$(1g^n_{9/2}$–$1h^p_{9/2})$	0.11
	$(1h^n_{11/2}$–$1i^p_{11/2})$	0.96
23.29	$(2f^n_{7/2}$–$2g^p_{7/2})$	0.23
	$(1g^n_{9/2}$–$1h^p_{9/2})$	0.13

Table 6. The microscopic structure of the spectrum in figure 3.

ω_i (MeV)	Structure	ψ^i_{np}
18.47	$(2f^n_{5/2}$–$3d^p_{5/2})$	−0.99
19.09	$(3p^n_{1/2}$–$4s^p_{1/2})$	−0.99
19.24	$(2d^n_{3/2}$–$3p^p_{3/2})$	−0.99
	$(1g^n_{9/2}$–$1h^p_{9/2})$	0.76
	$(2d^n_{5/2}$–$2f^p_{5/2})$	0.44
21.10	$(3p^n_{3/2}$–$3d^p_{3/2})$	0.40
	$(2f^n_{7/2}$–$2g^p_{7/2})$	−0.18
	$(1h^n_{11/2}$–$1i^p_{11/2})$	−0.13
	$(2f^n_{7/2}$–$2g^p_{7/2})$	0.95
22.38	$(1h^n_{11/2}$–$1i^p_{11/2})$	−0.27
	$(31g^n_{9/2}$–$1h^p_{9/2})$	0.10
	$(1h^n_{11/2}$–$1i^p_{11/2})$	0.94
23.47	$(2f^n_{7/2}$–$2g^p_{7/2})$	0.23
	$(2g^n_{7/2}$–$3f^p_{7/2})$	0.18
	$(1g^n_{9/2}$–$1h^p_{9/2})$	0.12
23.59	$(2g^n_{7/2}$–$3f^p_{7/2})$	−0.98
	$(1h^n_{11/2}$–$1i^p_{11/2})$	0.17

the calculations have been based on the assumption that the relativistic matrix elements are proportional to the non-relativistic one. Furthermore, the β decay $\log ft$ values for $0^+ \leftrightarrow 0^-$ transitions have been calculated and the influence of the effective interaction in the *pp* channel on the $\log ft$ values has been studied for the nuclei in the mass region of $90 \leq A \leq 214$.

The following conclusions may be drawn from our calculations:

(1) The relativistic matrix elements calculated in the first approximation are 2–5 times larger than those calculated in the second one.

(2) The *pp* effective interaction has no significant effect on the velocity of $0^+ \leftrightarrow 0^-$ transitions.

(3) While the relativistic matrix elements calculated according to the first approximation for heavier nuclei in the investigated mass region show a good agreement with the corresponding experimental data, this agreement for the light mass nuclei seems in the calculations performed according to the second approximation.

(4) The calculated energies of FFR for $^{210-214}$Pb isotopes are in agreement with the experimental values and the results of theoretical calculations.

References

[1] I N Borzov, *Nucl. Phys.* **A777**, 645 (2006)
[2] I N Borzov, *Phys. Rev.* **C67**, 025802 (2003)
[3] I N Borzov, *Nucl. Phys.* **A718**, 635c (2003)
[4] F Simkovic, private communication
[5] C Barbero *et al*, *Phys. Lett.* **B345**, 192 (1995)
[6] H F Schopper, *Weak interactions and nuclear beta decay* (North-Holland, Amsterdam, 1966)
[7] W C Haxton and G J Stephenson Jr., *Prog. Part. Nucl. Phys.* **12**, 409 (1984)
[8] C Barbero *et al*, *Phys. Lett.* **B436**, 49 (1998)
[9] O Civitarese and J Suhonen, *Nucl. Phys.* **A607**, 152 (1996)
[10] S Unlu *et al*, FINUSTAR, Greece, 12–17 September (2005)
[11] O Civitarese *et al*, *Nucl. Phys.* **A453**, 45 (1986)
[12] J Suhonen, *Nucl. Phys.* **A563**, 205 (1993)
[13] H De Witte *et al*, *Phys. Rev.* **C69**, 044305 (2004)
[14] E K Warburton *et al*, *Phys. Rev.* **C49**, 824 (1994)
[15] P Baumann *et al*, *Phys. Rev.* **C58**, 1970 (1998)
[16] I Kenar *et al*, *Math. Comp. Appl.* **10(2)**, 179 (2005)
[17] I Kenar *et al*, *Math. Comp. Appl.* **13(1)**, 1 (2008)
[18] A Bohr and B R Mottelson, *Nuclear structure* (W A Benjamin, Inc., New York, 1969) Vol. 1
[19] V G Soloviev, *Theory of complex nuclei* (Pergamon, New York, 1976)
[20] B Singh *et al*, *Nuclear Data Sheets* **84**, 487, DS980015 (1998)
[21] D J Horen *et al*, *Phys. Lett.* **B95**, 27 (1980)
[22] D J Horen *et al*, *Phys. Lett.* **B99**, 383 (1981)